

1 **Effect of gel formation on the dissolution behavior of clarithromycin tablets**

2

3 Koki Inukai<sup>a</sup>, Kei Takiyama<sup>a</sup>, Shuji Noguchi<sup>a,b</sup>, Yasunori Iwao,<sup>a</sup> Shigeru Itai<sup>a,\*</sup>

4

5 <sup>a</sup>*Department of Pharmaceutical Engineering, Graduate School of Pharmaceutical Sciences,*

6 *University of Shizuoka, 52-1 Yada, Suruga-ku, Shizuoka 422-8526, Japan*

7 <sup>b</sup>*Faculty of Pharmaceutical Sciences, Toho University, 2-2-1 Miyama, Funabashi, Chiba 274-8510,*

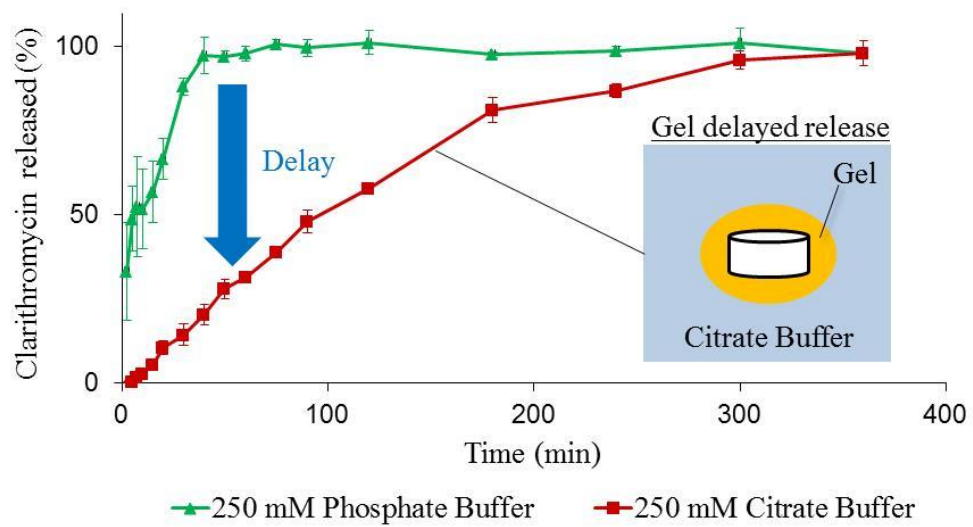
8 *Japan*

9

10 Abbreviations: CAM, clarithromycin; HPLC, high-performance liquid chromatography; PXRD,

11 powder X-ray diffraction; DSC, differential scanning calorimetry.

12



Graphic abstract

13

14

15 **Abstract**

16 Clarithromycin (CAM) is a macrolide antibiotic that is widely used at clinical sites. We found that  
17 release of CAM is suppressed when tablets of CAM were exposed to an external solvent containing  
18 carboxylate buffers such as citrate. The suppressed release of CAM can be attributed to the  
19 formation of gels on the tablet surfaces, which inhibits penetration of the solvent into the tablet and  
20 thus disintegration of the tablets. Delayed disintegration of the tablets was also observed for  
21 commercial tablets. This suggests that taking CAM and carboxylates at the same time might be  
22 avoided. The crystal structure of CAM citrate reveals that molecular chains of CAM are cross-linked  
23 by hydrogen bond between citrate groups in the crystal. The crystal structure indicates that  
24 cross-linked CAM chains of the three-dimensional mesh structure might also be formed in high  
25 concentration CAM solutions in the presence of carboxylates, resulting in gel formation.

26

27

28 **Keywords:** Clarithromycin, Single-crystal X-ray diffraction, Gelation, Carboxylate buffer

29

## 30 **1. Introduction**

31 Clarithromycin (CAM) is a 14-membered-ring macrolide antibiotic with a broad antibacterial  
32 spectrum, and it is widely used for the clinical treatment of various infectious diseases. It is used, as  
33 first-line drug even in today (Judith et al., 2016), with amoxicillin and a proton pump inhibitor to  
34 eradicate *Helicobacter pylori*, which was reported to cause stomach cancer.

35 The dissolution rate of CAM is affected by polymorphic transitions. When a CAM tablet  
36 consisting of form I crystals is exposed to an external solution, fine-needle-shaped form IV crystals  
37 spontaneously form and cover the tablet surfaces. This coating of form IV crystals prevents the  
38 solution from penetrating into the tablet, which inhibits disintegration of the tablet and suppresses  
39 release of CAM (Fujiki et al., 2011 and 2015). Noguchi et al. (2014) found that under acidic  
40 conditions containing hydrochloride, form II CAM transforms to a chloride salt crystal with a higher  
41 dissolution rate via a gel and a metastable crystalline form. In their study, release of CAM was also  
42 found to be delayed when a tablet consisting of form II crystals was exposed to an external solvent  
43 containing carboxylates. Carboxylates are often contained in foods. For example, vinegar contains  
44 approximately 5% acetate (800 mM), and grapefruit juice and orange juice contain approximately  
45 130 and 90 mM citrate, respectively (Penniston et al., 2008). CAM is generally taken after a meal,  
46 and its dissolution might be affected by carboxylates contained in food and drink. Floating  
47 gastroretentive drug delivery systems of CAM have been reported, which reside in the stomach and  
48 release CAM in a sustained manner for efficient eradication of *H. pylori* (Aoki et al., 2015;  
49 Rajinikanth et al., 2008), and their function would be also disrupted by carboxylates because the gel  
50 formed with carboxylates would change the particle density and suppress the releases of drugs. The  
51 suppression of drug releases by gels formed with polymers has been applied to the controlled  
52 releases of drugs: for recent example using  $\beta$ -glucans (Xiaoju et al., 2016) and the mixture of  
53 hydroxypropyl methylcellulose and hydroxypropyl cellulose (Hien et al., 2016). However, controlled

54 release by gels formed with citrate, a low molecular-weight excipient, has not been reported.

55 In this paper, the dissolution behavior of CAM in buffers containing carboxylates is reported,  
56 and the possible interaction between CAM and citrate (a carboxylate) is discussed based on the  
57 crystal structure of CAM citrate.

58

## 59 **2. Materials and methods**

### 60 *2.1. Materials*

61 Form II CAM was purchased from Shiono Chemical Co., Ltd. (Tokyo, Japan). All of the other  
62 reagents used were of the highest grade available from commercial sources.

63

### 64 *2.2. Preparation of CAM tablets*

65 Form II CAM powder 67 wt%, Perfiller 101 32 wt%, and magnesium stearate 1 wt% were  
66 mixed with a V-shape rotating mixer at 35 rpm for 5 min. The mixed powder (200 mg) was then  
67 tableted by a TabAll N30-EX single-punch tablet machine (Okada Seiko Company, Ltd., Tokyo,  
68 Japan) using an 8 mm diameter flat-faced punch with a tableting force of 10 kN.

69

### 70 *2.3. Disintegration and dissolution testing of tablets*

71 The disintegration tests were performed according to the method described in JP XVII. The  
72 times taken for complete disintegration of the tablets were measured using an NT-1HM  
73 disintegration tester (Toyama Sangyo Company, Ltd., Osaka, Japan) ( $n=6$ ). The solvents used were  
74 25 and 250 mM sodium phosphate buffer (PB), 25, 50, 75, 100, and 250 mM sodium citrate buffer  
75 (CB), and 75, 100, 150, 200, and 250 mM sodium acetate buffer (AB) ( $37.0 \pm 0.5$  °C). The pH  
76 values of the solvents were adjusted to 5.0, taken the pH value in the stomach after meals or  
77 administration of a proton pump inhibitor into consideration.

78 The dissolutions tests were performed according to the paddle method in JP XVII. The solvents  
79 were the same as those used in the disintegration tests and their volumes were 900 mL. The  
80 temperature was maintained at  $37.0 \pm 0.5$  °C and the paddle speed was 50 rpm. Aliquots of the  
81 solution (1.5 mL) were removed at predetermined time intervals, and then filtered through a 0.20 µm  
82 membrane filter. The CAM concentration was quantified by a high-performance liquid  
83 chromatography (HPLC) system consisting of a Shimadzu LC-9A pump, a Shimadzu SPD-6A UV  
84 spectrophotometric detector, a Shimadzu CTO-6A column oven, a Shimadzu SIL-6B autoinjector,  
85 and a Shimadzu Chromatopac C-R7A plus data processor (Shimadzu Corp., Tokyo, Japan). The  
86 operating conditions were as follows: an ultraviolet absorption photometer wavelength of 210 nm, a  
87 4.6 mm internal diameter x 15 cm stainless-steel column packed with octadecyl silica (ODS)-80TM  
88 (Tosoh Co., Tokyo, Japan), a column temperature of 40 °C, a mixture of 1/15 M potassium  
89 dihydrogen phosphate and acetonitrile (13:7) as the mobile phase, and a flow rate of 1 mL/min.

90

#### 91 *2.4. Dissolution testing by the static disc method*

92 Crystal powder of form II CAM (250 mg) was compressed into 13 mm diameter disks using an  
93 oil-press tableting machine (JASCO Corporation, Tokyo, Japan) with a tableting force of 10 kN. The  
94 CAM disks were fixed into a cylindrical holder. The surface area of the disk in contact with the  
95 dissolution medium was 1.33 cm<sup>2</sup>. The holder was placed in a bottle containing 900 mL of the  
96 dissolution medium and allowed to sink to the bottom, according to JP XVII. All of the dissolution  
97 tests were performed under the sink condition. The medium was stirred with a paddle at 50 rpm  
98 according to the paddle method of JP XVII. The solvents were 25 mM PB and 1, 25, or 250 mM CB  
99 containing 25 mM PB ( $37.0 \pm 0.5$  °C). The solvents were adjusted to pH 5.0. The dissolved CAM  
100 concentrations were quantified by HPLC, as described in Section 2.3.

101 The solvents, as specified in Section 2.3, and excess crystal powder of form II CAM were

102 added to 2 mL tubes with screw caps. The tubes were mixed upside down in an incubator at  $37 \pm$   
103  $0.5$  °C. The solutions were filtered after 1 h and diluted ten-fold with the same solvents, and their  
104 CAM concentrations were quantified by HPLC, as described at Section 2.3. The measured  
105 concentrations were the same as those measured by the same procedure after 1.5 h, confirming that  
106 the CAM concentration reached the saturated concentration.

107 The apparent intrinsic dissolution rate  $k$  ( $\text{cm min}^{-1}$ ) was calculated using the following  
108 equation:

$$109 \quad k = KV/(SC_S) \quad (1)$$

110 where  $K$  is the dissolution rate,  $V$  is the volume of the dissolution medium,  $S$  is the surface area in  
111 contact with the dissolution medium, and  $C_S$  is the solubility.

112

### 113 *2.5. Preparation of CAM carboxylate salts*

114 Crystal powder of form II CAM (250 mg) and distilled water (70 mL) were mixed with a  
115 stirring bar in a beaker, and CAM was dissolved by decreasing the pH to 5.0 using 5 M phosphoric  
116 acid solution. Undissolved CAM was removed with filter paper. The filtrates were mixed with 105  
117 mL of 3.0 M AB (pH 5.0), 0.7 mL of 1.0 M CB, 12.3 mL of sodium malate buffer, 14 mL of 0.5 M  
118 sodium tartrate buffer, or 21 mL of 0.2 M sodium oxalate buffer. The solutions were stirred  
119 overnight at room temperature. The precipitates or gel formed were collected using a Buchner funnel  
120 and filter paper, and they were washed with distilled water. The collected samples were dried for 2  
121 days at 37 °C.

122

### 123 *2.6. X-ray powder diffraction analysis*

124 The powder X-ray diffraction (PXRD) data of the CAM carboxylate salts was collected at beam  
125 line BL5S2 of the Aichi Synchrotron Radiation Center, which is equipped with a Debye–Sherrer

126 camera and a curved imaging plate detector. The salt powders were packed in 0.4 mm diameter  
127 Lindemann glass capillaries. The X-ray wavelength was set to 1.000 Å and the temperature was  
128 25 °C.

129

### 130 *2.7. Differential scanning calorimetry*

131 Differential scanning calorimetry (DSC) measurements of the CAM carboxylate salts were  
132 performed using a DSC7020 calorimeter (Hitachi High-Tech, Tokyo, Japan) at a heating rate of  
133 10 °C min<sup>-1</sup> under 40 mL min<sup>-1</sup> dry N<sub>2</sub> gas.

134

### 135 *2.8. Single-crystal X-ray structure analysis of CAM citrate*

136 Crystal powder of CAM citrate was prepared (see Section 2.5). A CAM citrate solution was  
137 made to dissolve this powder and citric acid powder in water, where the amount was controlled by  
138 reducing the pH to 3.6 using a pH meter. The beaker containing the saturated solution (about 10 mL)  
139 was placed in an enclosed space with calcium chloride. The solution slowly evaporated at room  
140 temperature. After 2 weeks, the solution was completely dry, and there were many plate-like crystals  
141 at the bottom of the beaker. These crystals were hermetically stored at room temperature.

142 Single-crystal X-ray diffraction data of CAM citrate was collected at beam line BL2S1 of the  
143 Aichi Synchrotron Radiation Center, which is equipped with an oscillation camera and an ADSC  
144 Quantum 315r charge-coupled device detector. The wavelength was set to 1.000 Å. During the data  
145 collection, the samples were cooled to 100 K using N<sub>2</sub> gas. The crystal parameters, statistics of the  
146 X-ray diffraction data collection, and crystallographic refinement data are summarized in Table 1.

147 The structure solution was performed using SHELXT (Sheldrick, 2015), and the structure was  
148 crystallographically refined using SHELXL (Sheldrick, 2015) and shelXle (Hübschle et al., 2011).

149 The atomic coordinates and diffraction data have been deposited in the Cambridge Structural



150 Database (CCDC number 1465268). The molecular structure and molecular sequence were  
151 determined using Mercury (Macrae et al., 2008).

152

### 153 *2.8. Disintegration testing of commercial CAM tablets*

154 Disintegration tests were performed according to JP XVII using commercial CAM tablets. The  
155 times taken for complete disintegration of the tablets were measured using an NT-1HM  
156 disintegration tester (Toyama Sangyo Company Ltd., Osaka, Japan) in triplicate at  $37.0 \pm 0.5$  °C.  
157 The solvents used were 25 and 250 mM of pH 5.0 PB and 25, 50, 75, 100, and 250 mM of pH 5.0  
158 CB.

159

## 160 **3. Results and discussion**

### 161 *3.1. Disintegration tests*

162 In disintegration tests using PB as the solvent, CAM tablets rapidly disintegrated: the maximum  
163 disintegration time was only 0.5 min in 250 mM buffer (Fig. 1). However, for buffers containing  
164 carboxylates, the disintegration times increased as the buffer concentration increased: the  
165 disintegration times in 250 mM AB and CB were approximately 500- and 300-times longer than that  
166 in PB. When CAM tablets were placed in 250 mM pH 5.0 AB, a translucent gel formed on the  
167 surface of the CAM tablets, as shown in Fig. 2. A gel also formed when CB was used, although it  
168 was less noticeable. The gels formed on the tablet surfaces may inhibit penetration of the solvent  
169 into the tablets, which results in inhibition of the disintegration of the tablets.

170

### 171 *3.2. Dissolution tests*

172 Dissolution tests were performed using sodium phosphate and carboxylate buffers (Fig. 3).  
173 Release of CAM was very rapid in the PB and 100% of CAM was released. In contrast, release of

174 CAM was suppressed in CB with concentrations higher than 50 mM and in the AB with  
175 concentrations higher than 200 mM. Release of CAM was suppressed more as the buffer  
176 concentration increased. In the sodium carboxylate buffers, the suppressed release of CAM can be  
177 attributed to inhibition of disintegration of the tablets caused by gel formation on the tablet surfaces.  
178 In the dissolution tests in the PB, the time to reach 100% CAM dissolution in 250 mM buffer was 20  
179 min longer than that in 25 mM buffer. This may be caused by the salting-out effect.

180

### 181 *3.3. Dissolution parameters*

182 The apparent intrinsic dissolution rates were calculated using the solubility of CAM and the  
183 dissolution rate from the disk of form II CAM (Table 2). The dissolution rate and solubility using 25  
184 mM CB are more than twice those using 1, or 250 mM CB. The difference in the solubility may be  
185 caused by salting-in and salting-out effects. The apparent intrinsic dissolution rate is significantly  
186 lower when 250 mM CB was used. This indicates that the decreased dissolution rate in 250 mM CB  
187 is not only caused by the decreased solubility. The gel formed on the surface of the disk may have  
188 inhibited CAM dissolution from the disk. There are three factors that may inhibit dissolution of  
189 CAM: inhibition of disintegration of the tablet, suppression of CAM elution by gel formation, and  
190 decrease in the solubility by the salting-out effect. Therefore, foods containing carboxylates,  
191 including citrate, may be avoided when taking CAM formulations, especially the floating  
192 gastroretentive drug delivery system.

193

### 194 *3.4. Evaluation of the physical and chemical properties of CAM carboxylate salts*

195 When sodium carboxylate buffer was added to CAM dissolved in PB, a gel immediately  
196 formed and the solution became cloudy. A photograph of the gel collected from the solvent using  
197 AB is shown in Fig. 4. A gel was formed using sodium citrate, malate, oxalate, and tartrate buffers.

198 PXRD profiles of the CAM carboxylate salts are shown in Fig. 5. All of the profiles are  
199 different from previously reported profiles of CAM, indicating that these are new crystals of  
200 carboxylate salts. The lattice constants and possible space groups of crystals prepared using AB and  
201 CB were calculated from the PXRD profiles using EXPO2014 (Table 3). All of the peaks in the  
202 PXRD profiles could be indexed with these cell parameters, confirming that each of these crystal  
203 powders consisted of a single crystalline phase. The crystal powder prepared using CB was  
204 confirmed to be CAM citrate hydrate by single-crystal X-ray structure analysis. Assuming that the  
205 crystals prepared using AB are CAM acetate and their space group is monoclinic  $P2_1$ , its specific  
206 volume (volume per unit molecular weight) is  $1.44 \text{ \AA}^3/\text{Da}$ . This value is comparable with the values  
207 of previously reported CAM crystals (Noguchi et al., 2014), suggesting that this crystal is CAM  
208 acetate or possibly CAM acetate hydrate. The diffraction peaks of the PXRD profiles of crystals  
209 prepared using malate, oxalate, and tartrate buffers could not be indexed using a single crystal cell,  
210 suggesting that these crystals are mixtures of polymorphs and/or pseudopolymorphs, such as  
211 hydrates.

212 The CAM carboxylate crystals were analyzed by DSC (Fig. 6). The melting points are  $226.4 \text{ }^\circ\text{C}$   
213 for form II,  $218.6 \text{ }^\circ\text{C}$  for the acetate salt,  $175.2 \text{ }^\circ\text{C}$  for the citrate salt,  $199.6 \text{ }^\circ\text{C}$  for the malate salt,  
214  $186.5 \text{ }^\circ\text{C}$  for the tartrate salt, and  $191.3 \text{ }^\circ\text{C}$  the tartrate salt. The differences in the melting points  
215 show that these are new crystal forms. All of the melting points of the CAM carboxylate salts are  
216 lower than that of form II. Although the melting points of the citrate and acetate salts are sharp  
217 endothermic peaks, those of the malate, oxalate and tartrate salts are not. This may be because the  
218 citrate and acetate salts are pure crystalline phase and the others are not, as suggested by PXRD  
219 analysis.

220

221 *3.5. Single-crystal X-ray structure analysis of CAM citrate*

222 Single-crystal structure determination of CAM citrate revealed that the unit cell consists of one  
223 CAM molecule, one citrate molecule, and five water molecules (Table 1). The occupancies of the  
224 four water molecules are less than 1.0.

225 The numbering of the atoms in the crystal structure is given in Fig. 7(a). A hydrogen-bonded  
226 network forms between CAM citrate and the water molecules (Fig. 7(b)). There is also a hydrogen  
227 bond between the O9 oxygen atom of the cladinose ring and the O3 oxygen atom of the  
228 14-membered aglycone ring of CAM molecules. The CAM molecules form in head-to-tail chain  
229 parallel to the *b* axis. This chain arrangement mediated by O9–O3 hydrogen bonds is also found in  
230 the crystal structures of form 0 (Spanton et al., 1999), metastable form I (Noguchi et al., 2012), and  
231 the hydrochloride hydrate (Parvez et al., 2000), suggesting that this arrangement is stable for CAM.  
232 Hydrogen bonds form between CAM and citrate parallel to the *c* axis between the protonated N1  
233 nitrogen atom of the CAM desosamine ring and the O16 hydroxyl oxygen of citrate, and parallel to  
234 the *b* axis between the O13 hydroxyl oxygen atom of the CAM desosamine ring and the O14  
235 carbonyl oxygen atom of citrate. Protonation of N1 is confirmed because the electron density of the  
236 hydrogen atom bound to N1 is clearly observed. The molecular chains of CAM are cross-linked by  
237 hydrogen bonds with citrate molecules. One of the carboxyl groups of the citrate molecule (O19–  
238 C43–O20) is thought to be deprotonated and O20 would have a negative electrostatic charge. This is  
239 because the O19–C43 and O20–C43 distances are 1.216 and 1.273 Å, indicating that they are double  
240 and single bonds, respectively, and O20 is a hydrogen acceptor for hydrogen atoms attached to the  
241 OW1 oxygen atom of a water molecule and the O15 carboxyl oxygen atom of a citrate molecule.  
242 The presence of the hydrogen atoms bound to OW1 and O15 is confirmed by the fact that their  
243 electron densities are clearly observed. These hydrogen bonds would stabilize the negatively charged  
244 O20 oxygen atom. No ionic bond is formed between CAM and citrate molecules, although they are  
245 positively and negatively charged, respectively. The other two carboxyl groups of the citrate

246 molecule (O15–C39–O16 and O17–C44–O18) are thought to be protonated, because the electron  
247 densities of hydrogen atoms bound to O15 and O18 are observed.

248 Although the structural characteristics described above are found in the crystal structure of  
249 CAM citrate, they also indicate the structure of the CAM gel formed in the buffer-containing  
250 carboxylate buffers. In the CAM citrate crystal, molecular chains of CAM are cross-linked by citrate  
251 molecules by a number of hydrogen bonds. These hydrogen bonds would also possibly form in the  
252 gel. The molecular chains of CAM might form at the region of high CAM concentration and the  
253 chain might be cross-linked by hydrogen bonds when carboxylates, such as citrate, coexist, as  
254 observed in the crystal structure. This results in formation of a three-dimensional mesh structure.  
255 Water molecules would be trapped in the mesh by formation of hydrogen bonds, as is observed in  
256 the crystal structure, and gelation would occur (Fig. 8). Controlled release of other weakly-basic  
257 drugs might be possible when the drugs are inclined to form gels with carboxylates as in the case of  
258 CAM.

259

### 260 *3.6. Disintegration testing of commercial CAM tablets*

261 In disintegration tests using PB as the solvent, commercial CAM tablets disintegrated and the  
262 maximum disintegration time was only 10 min (Fig. 9). In disintegration tests using CB as the  
263 solvent, the tablets rapidly disintegrated in 25 and 50 mM buffer solutions. However, the  
264 disintegration time increased with increasing concentration of the buffer for concentrations higher  
265 than 50 mM. The maximum disintegration time was 340.4 min in 250 mM CB. It is assumed that  
266 penetration of the solvent into the tablet is suppressed by the gel formed on the tablet surface, as  
267 discussed in Section 3.1. These results suggested that the disintegration time of commercial tablets  
268 could significantly increase in the presence of carboxylates, for example, by more than 2 h in 100  
269 mM citrate, which is the typical concentration in citrus juices. It is assumed that disintegration and

270 dissolution of CAM are also delayed with intake of citric acid from foods.

271

#### 272 **4. Conclusion**

273 Disintegration and dissolution tests using AB and CB showed that dissolution of CAM is  
274 suppressed depending on their concentration, because a gel formed on the tablet surfaces would  
275 delay disintegration. Disintegration of commercial tablets was also delayed in CB. Hence, foods and  
276 drinks with high carboxylate contents, such as grapefruit juice, might be avoided when taking CAM  
277 formulations, especially the floating gastroretentive drug delivery system.

278 Single-crystal X-ray structure analysis of CAM citrate revealed that molecular chains of CAM  
279 are cross-linked by hydrogen bonds between citrate molecules in the crystal. It is assumed that these  
280 molecular chains of CAM might be also formed in the gel. The molecular chains of CAM might be  
281 cross-linked by hydrogen bonds when carboxylates, such as citrate, are present, similar to the crystal  
282 structure, resulting in formation of a three-dimensional mesh structure.

283

#### 284 **Acknowledgments**

285 The synchrotron radiation experiments were performed at beam lines BL5S2 and BL2S1 of the  
286 Aichi Synchrotron Radiation Center, Aichi Science & Technology Foundation, Aichi, Japan  
287 (approval numbers 201401010, 201403031, and 2015N2011). This work was supported by the Japan  
288 Society for the Promotion of Science KAKENHI (grant numbers 26460224, 26460039, and  
289 26460226).

290

291 **References**

- 292 Aoki, H., Iwao, Y., Mizoguchi, M., Noguchi, S., Itai, S., 2015. Clarithromycin highly-loaded  
293 gastro-floating fine granules prepared by high-shear melt granulation can enhance the efficacy  
294 of *Helicobacter pylori* eradication. *Eur. J. Pharm. Sci.* 92, 22–27.
- 295 Altomare, A. Cuocci, C. Giacobozzo, C. Moliterni, A. Rizzi, R. Corriero N., Falcicchio, A., 2013.  
296 EXPO2013: a kit of tools for phasing crystal structures from powder data. *J. Appl. Crystallogr.*  
297 46, 1231–1235.
- 298 Fujiki, S., Iwao, Y., Kobayashi, M., Miyagishima, A., Itai, S., 2011. Stabilization mechanism of  
299 clarithromycin tablets under gastric pH condition. *Chem. Pharm. Bull.* 59, 553–558.
- 300 Fujiki, S., Watanabe, N., Iwao, Y., Noguchi, S., Mizoguchi, M., Iwamura, T., Itai, S., 2015.  
301 Suppressed release of clarithromycin from tablets by crystalline phase transition of metastable  
302 polymorph form I. *J. Pharm. Sci.* 104, 2641–2644.
- 303 Hien, V. N., Van, H., N., Beom, J., L., 2016. Dual release and molecular mechanism of bilayered  
304 aceclofenac tablet using polymer mixture. *Int. J. Pharm.* 515, 233–244.
- 305 Hübschle, C.B., Sheldrick, G.M., Dittrich, B., 2011. ShelXle: a Qt graphical user interface for  
306 SHELXL. *J. Appl. Crystallogr.* 44, 1281–1284.
- 307 Noguchi, S., Miura, K., Fujiki, S., Iwao, Y., Itai, S., 2012. Clarithromycin form I determined by  
308 synchrotron X-ray powder diffraction. *Acta Crystallogr. C* 68, 41–44.
- 309 Noguchi, S., Takiyama, K., Fujiki, S., Iwao, Y., Miura, K., Itai, S., 2014. Polymorphic transformation  
310 of antibiotic clarithromycin under acidic condition. *J. Pharm. Sci.* 103, 580–586.
- 311 Macrae, C.F., Bruno, I.J., Chisholm, J.A., Edgington, P.R., McCabe, P., Pidcock, E.,  
312 Rodriguez-Monge, L., Taylor, R., van de Streek, J., Wood, P.A., 2008. Mercury CSD 2.0 -  
313 New Features for the visualization and investigation of crystal structures. *J. Appl. Cryst.* 41,

314 466–470.

315 Parsons, S., Flack, H.D., Wagner, T., 2013. Use of intensity quotients and differences in absolute  
316 structure refinement. *Acta Crystallogr. B*69, 249–259.

317 Parvez, M., Arayne, M.S., Sabri, R., Sultana, N., 2000. Clarithromycin hydrochloride 3.5-hydrate.  
318 *Acta Crystallogr. C*56, 398–399.

319 Penniston, K.L., Nakada, S.Y., Holmes, R.P., Assimos, D.G., 2008. Quantitative assessment of citric  
320 acid in lemon juice, lime juice, and commercially-available fruit juice products. *J.*  
321 *Endourology* 22, 567–570.

322 Rajinikanth, P.S., Mishra, B., 2008. Floating in situ gelling system for stomach site-specific delivery  
323 of clarithromycin to eradicate *H. pylori*. *J. Controlled Release*. 125, 33–41.

324 Sheldrick, G.M., 2015. Crystal structure refinement with *SHELXL*. *Acta Crystallogr. C*71, 3–8.

325 Sheldrick, G.M., 2015. *SHELXT* – Integrated space-group and crystal-structure determination. *Acta*  
326 *Crystallogr. A*71, 3–8.

327 Spanton, S.G., Henry, R.F., Riley, D.A., Liu, J.-H., 1999. Crystal form O of clarithromycin. US  
328 Patent No. 5945405.

329 Xiaoju, Z., Pengyu, W., Jiong, W., Zhi, L., Xuechuan, H., Yuling, X., Peng, L., Xianming, H., 2016.  
330 Hydroxyethyl Pachyman as a novel excipient for sustained-release matrix tablets. *Carbohydr.*  
331 *Polym.* 154, 1–7.

332 Judit, A., Gloria, F., Enoc, C., Carlos, A., C., Jose, D., S., Ivan, C., C., Reyes, B., Adolfo, R., 2016.  
333 Clarithromycin resistance and prevalence of *Helicobacter pylori* virulent genotypes in patients  
334 from Southern México with chronic gastritis. *Infect. Genet. Evol.* 44, 190–198.



335 **FIGURE CAPTIONS**

336 **Fig. 1.** Disintegration times in the carboxylate buffers. Each bare represents the mean  $\pm$  standard  
337 deviation (SD) ( $n=6$ ).

338 **Fig 2.** Gel of CAM formed on the form II tablet. The tablet was placed in 250 mM AB and stirred  
339 for 5 min at 37.0 °C.

340 **Fig 3.** CAM dissolution test results. Each data represents the mean  $\pm$  SD ( $n=3$ ).

341 **Fig 4.** Gel formed when CAM powders are mixed with AB.

342 **Fig 5.** PXRD profiles of CAM carboxylate salts. Form II (green), CAM acetate (blue), CAM citrate  
343 (red), CAM malate (purple), CAM oxalate (light green), and CAM tartrate (yellow).

344 **Fig 6.** DSC curves of CAM carboxylate salts. Form II (green), CAM acetate (blue), CAM citrate  
345 (red), CAM malate (purple), CAM oxalate (light green), and CAM tartrate (yellow).

346 **Fig 7.** (a) Molecular structures of CAM, citrate, and water molecules with the atom-numbering  
347 scheme. C, O, and N atoms are shown in grey, red, and light blue, respectively. (b) Crystal structure  
348 of CAM citrate. The unit cell is shown as a thin black line. CAM and citrate are shown in light blue  
349 and green, respectively. Hydrogen atoms are not shown for clarity. Hydrogen bonds are shown as  
350 black dotted lines.

351

352 **Fig 8.** Schematic drawing of the proposed structure of the CAM citrate gel. CAM and citrate are  
353 shown as blue and green spheres, respectively. Water molecules except for OW1 are not shown.

354

355 **Fig 9.** Disintegration times of commercial tablets in different concentration buffer solutions. Each

356 column represents the mean  $\pm$  SD ( $n=3$ ).

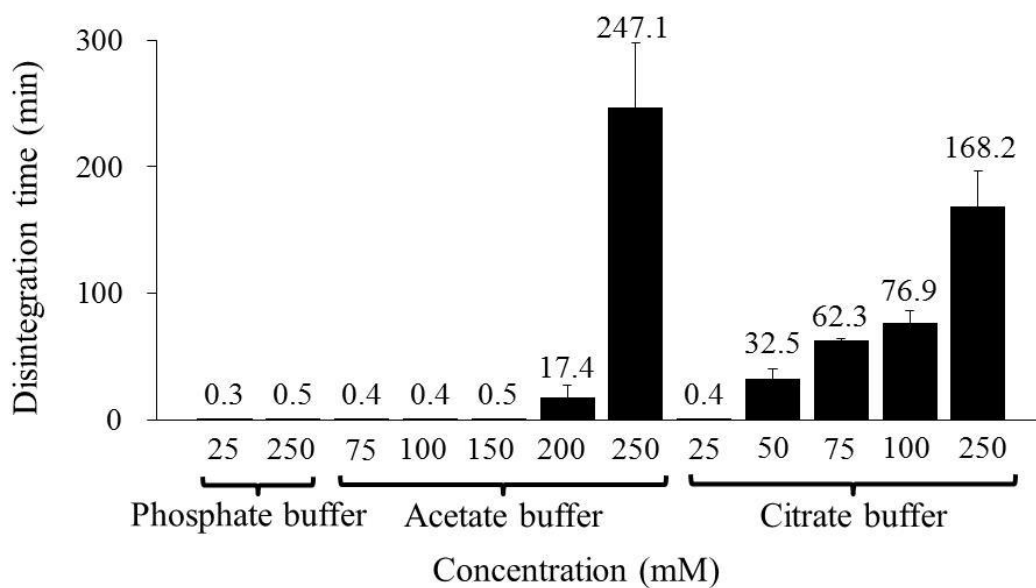


Fig. 1

357

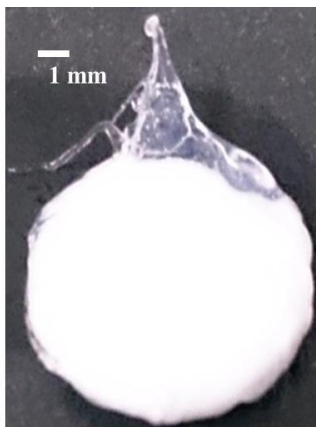


Fig. 2

358

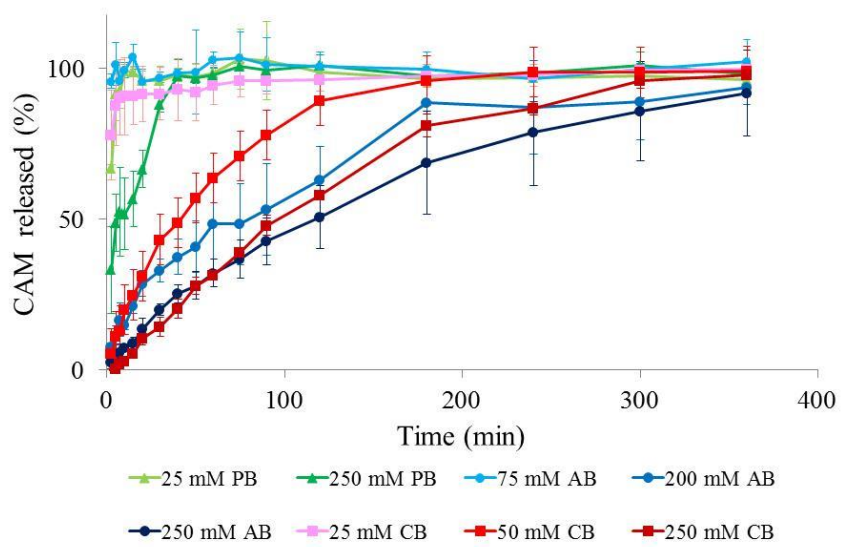


Fig. 3

359

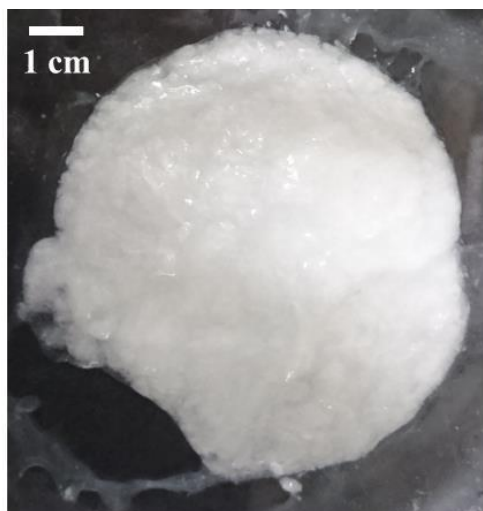


Fig. 4

360

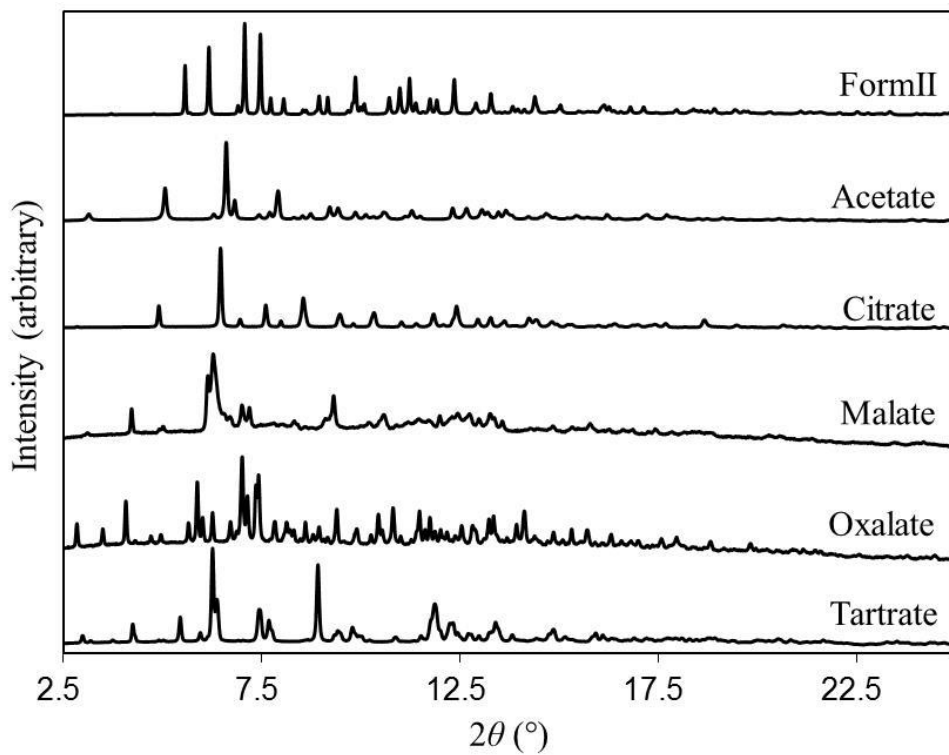


Fig. 5

361

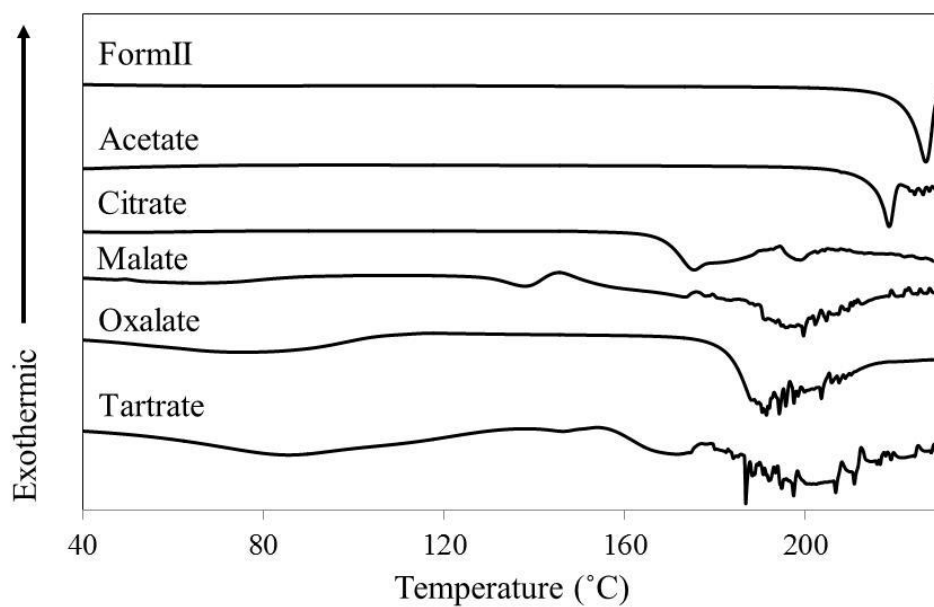


Fig. 6

362

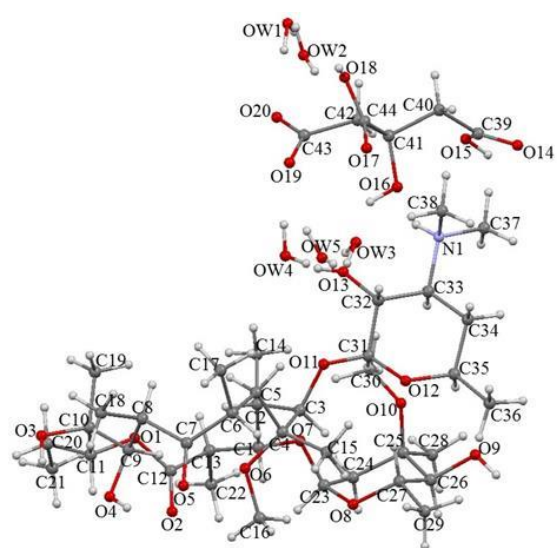


Fig. 7 (a)

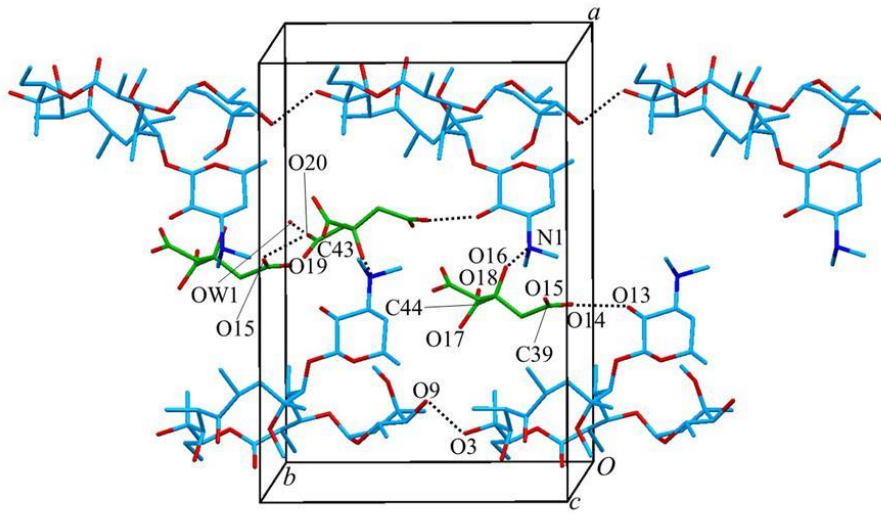


Fig. 7 (b)

364

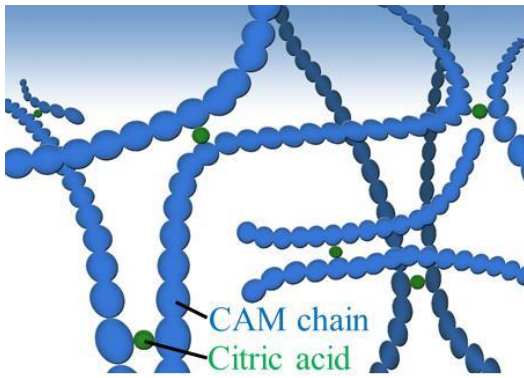


Fig. 8

365

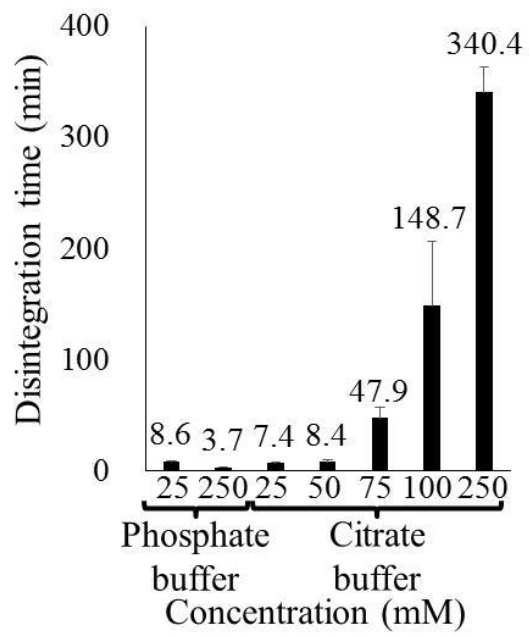


Fig. 9